J Seismol (2012) 16:745–755
DOI 10.1007/s10950-012-9304-9

ORIGINAL ARTICLE

Toroidal free oscillations of the Earth observed by a ring laser system: a comparative study

M. F. Nader · H. Igel · A. M. G. Ferreira · D. Kurrle · J. Wassermann · K. U. Schreiber

Received: 27 October 2011 / Accepted: 26 March 2012 / Published online: 10 May 2012

Abstract In this study, we explore the potential of measuring systematically the Earth's free oscillations using ring laser gyro (RLG) vertical axis rotational records. The RLG that we use is the vertical axis G-ring laser system of the Geodetic Observatory Wettzell (Germany). In 2009, its signal-to-noise ratio was considerably improved over the broadband frequency range of seismic measurements. Since then, three large magnitude earthquakes have occurred (Samoa Islands 2009; Maule, Chile, 2010; and Tohoku, Japan, 2011), leading to the first direct observations of rotational ground motions induced by toroidal free oscillations of the Earth. We compare these G-ring laser observations with synthetic seismograms computed by summing normal modes. We also analyse amplitude spectra of real and synthetic data to aid in the interpretation of the observations. We show that several toroidal modes are detected by the G-ring laser for earthquakes with a moment magnitude $M_W \geq 8.0$ and that our observations are in reasonable agreement with the synthetic spectra. We also report evidence for mode coupling in both translation and rotation spectra.

Keywords Free oscillations · Rotational seismology · Love waves

M. F. Nader (✉) · H. Igel · D. Kurrle · J. Wassermann
Department of Earth and Environmental Sciences,
Ludwig-Maximilians-University of Munich,
Theresienstr.41,
80333 Munich, Germany
e-mail: nader@geophysik.uni-muenchen.de

A. M. G. Ferreira
School of Environmental Sciences,
University of East Anglia,
Norwich NR4 7TK, UK

A. M. G. Ferreira
ICIST, Instituto Superior Técnico,
Technical University of Lisbon,
Lisbon, Portugal

D. Kurrle
Now at State Earthquake Service Baden-Württemberg,
Freiburg, Germany

K. U. Schreiber
Forschungseinrichtung Satellitengeodäsie,
Technical University of Munich,
Fundamentalstation Wettzell, Sackenriederstr. 25,
93444 Kötzting, Germany

1 Introduction

The Earth's free oscillations induced by large earthquakes have been one of the most important ways to measure the Earth's internal structure. They provide important large-scale constraints on a variety of elastic parameters, attenuation and density of the Earth's deep interior (for example, Gilbert and Dziewonski 1975; Giardini et al. 1987; Beghein and Trampert 2003; Deuss et al. 2010; Ishii and Tromp 1999; Laske and Masters 1999).

Very large earthquakes excite free oscillations significantly above our planet's background noise level. Nevertheless, correct, unambiguous observations of free oscillation spectra remain challenging, in particular for toroidal modes. The difficulty in the observation of toroidal modes results from (1) toroidal modes—the superposition of Love waves—have lower Q (higher attenuation) than spheroidal modes, so toroidal oscillations decay more rapidly; (2) measuring horizontal ground translations is more difficult due to the higher noise levels in the records of horizontal seismometers; and (3) the horizontal components of motions suffer from cross-coupling effects so that surface tilts can lead to apparent translational motions exceeding true translational motions (Widmer-Schnidrig and Zürn 2009). It is here where improvements and complements to existing techniques are helpful, and the contribution of rotational records in the study of Earth's free oscillations could play an important role.

Given sufficient sensitivity, rotational sensors can be used to observe toroidal modes directly by recording motions around a locally vertical axis with very low (theoretically zero) cross sensitivity to translational motions. Further, the quality of horizontal translational observations can be improved if the rotational motions (tilt around horizontal axes) can be corrected for.

Here we explore the potential of rotational measurements by high-precision ring laser gyros (RLG) systems for the study of long-period toroidal oscillations; we focus on the comparison of RLG observations of free oscillations caused by three recent, large earthquakes. We compare rotational seismograms recorded by the G-ring RLG to transverse acceleration records from a collocated STS-2 seismometer.

The paper begins with a brief presentation of the ring laser measurement principle after which we describe the three earthquakes we use. We present long-period data in both time and frequency domains, followed by comparison with synthetic seismograms and an analysis of the spatial motion pattern. Finally we discuss the possibility of Coriolis coupling between toroidal and spheroidal modes in both translation and rotation data.

2 Instrumentation

Several different instruments have been developed to measure the rotational part of a seismic wave field. So far, the most successful results—at least in broadband seismology—have been achieved using ring laser technology.

RLGs are active interferometers that are highly sensitive to rotations but highly insensitive to translations (zero sensitivity in the absence of structural distortions caused by translational motions). In the case of the G-ring laser in Wettzell (southern Bavaria, Germany; Fig. 1), the laser cavity is a square with an arm length of 4 m (area of 16 m^2).

The RLG has two counter propagating single-mode laser beams that are decoupled with respect to each other (by Earth rotation). Since the effective perimeter of the laser cavity differs minutely for the two directions of beam propagation, the beams are lasing at slightly different optical frequencies. When the beams are superimposed outside the cavity, one obtains an interferogram whose beat frequency (Sagnac frequency) is proportional to the rate of rotation about the axis perpendicular to the plane of the ring, so about the vertical axis. In the case of the G-ring, the laser cavity is filled with a helium–neon gas mixture and lases at 632.8 nm (Schreiber et al. 2006, 2009).

Since 2009, the use of highly polished super mirrors reduced the loss of the resonator to approximately 50 ppm. This made the sensor more sensitive and

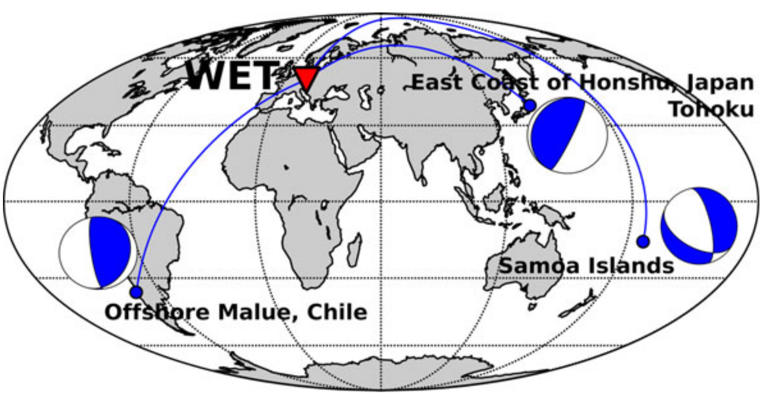

Fig. 1 Ring laser and broadband receiver location in Wettzell, Germany (*red triangle*) and epicentres and Global CMT source mechanisms of the three seismic events used in this study

Table 1 Global CMT catalogue parameters for the studied events

Event	Tohoku	Chile	Samoa
M_W	9.0	8.8	8.1
Date	11 March 2011	27 Feb 2010	29 Sept 2009
GMT time	5:47:32.8	6:35:14.5	17:48:26.8
Lat/Lon	37.5 N/143.0 E	35.9 S/73.1 W	15.1S/171.9W
Depth [km]	20.0	23.2	12.0

minimised the attenuation of the beam. Smaller loss translates into a narrower line width of the laser, a more stable frequency reference and consequently into lower sensor noise and higher resolution. Thanks to these improvements, the G-ring laser now resolves to a noise level of $\Delta\Omega = 1,2 \times 10^{-11}\mathrm{rad/s}/\sqrt{\mathrm{Hz}}$ for the continuous monitoring of the Earth's rotational ground motions. This very high sensitivity for the measurement of seismically induced rotational motions is now good enough to detect multiple-orbit surface waves, as discussed below.

Because it is sensitive to Z-axis rotations, the G-ring laser is primarily excited by horizontally polarised shear motions (SH waves, Love waves) and is insensitive to compressional waves and conversions (P-SV) and Rayleigh waves. Consequently, this instrument detects mostly toroidal modes (assuming that there is no tilt-

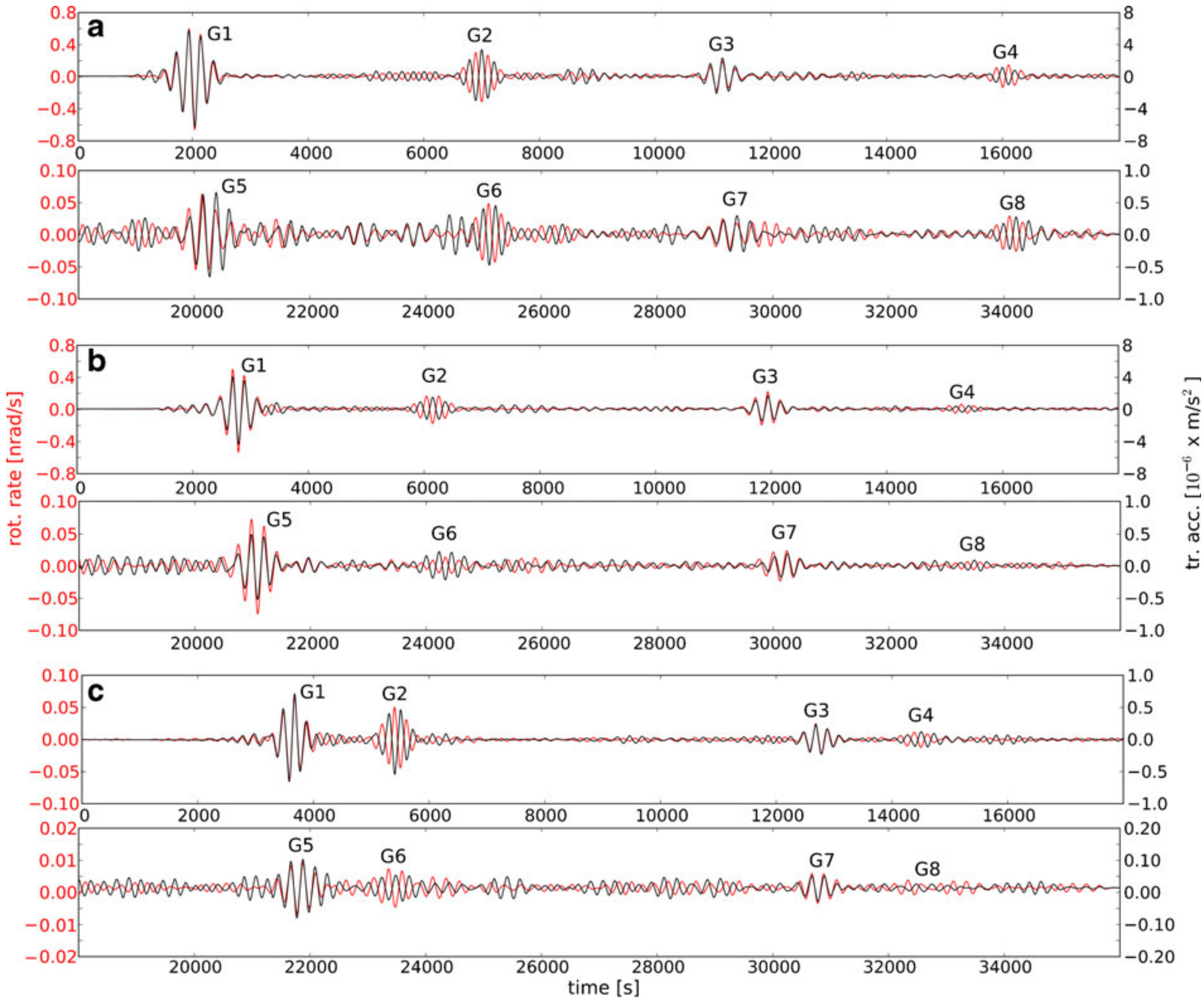

Fig. 2 Observed multiple-orbit Love waves for the **a** M_W 9.0 Tohoku (2011); **b** M_W 8.8 Maule, Chile (2010) and **c** M_W 8.1 Samoa earthquakes recorded in Wetzell, Germany. The rotation rate around the vertical axis is the *red trace* and *left axes* and transverse acceleration is the *black trace* and *right axes*. The traces are band-pass filtered between 180 and 280 s

to-laser coupling, which in general can be neglected; Pham et al. 2009), unless there is coupling between spheroidal and toroidal modes (Masters et al. 1983)

3 Observations and analysis

We report observations from three recent large earthquakes (Fig. 1 and Table 1). In temporal order, these are the M_W 8.1 Samoa islands earthquake of September 29, 2009; the M_W 8.8 earthquake off the coast of Maule, Chile on February 27, 2010; and the M_W 9.0 Tohoku earthquake of March 11, 2011.

3.1 Time-domain observations and modelling

Observations of both translational and rotational ground motions are shown in Fig. 2. The RLG seismograms were compared to transverse accelerations records of the collocated STS-2 seismometer (WET). Transverse accelerations were obtained by rotating the original seismograms into radial, transverse and vertical directions, correcting for instrument response and differentiating in time.

No instrument correction is necessary for the ring laser system because it has a flat response. As explained in other studies (Pancha et al. 2000; Igel et al. 2007; Ferreira and Igel 2009; and Kurrle et al.

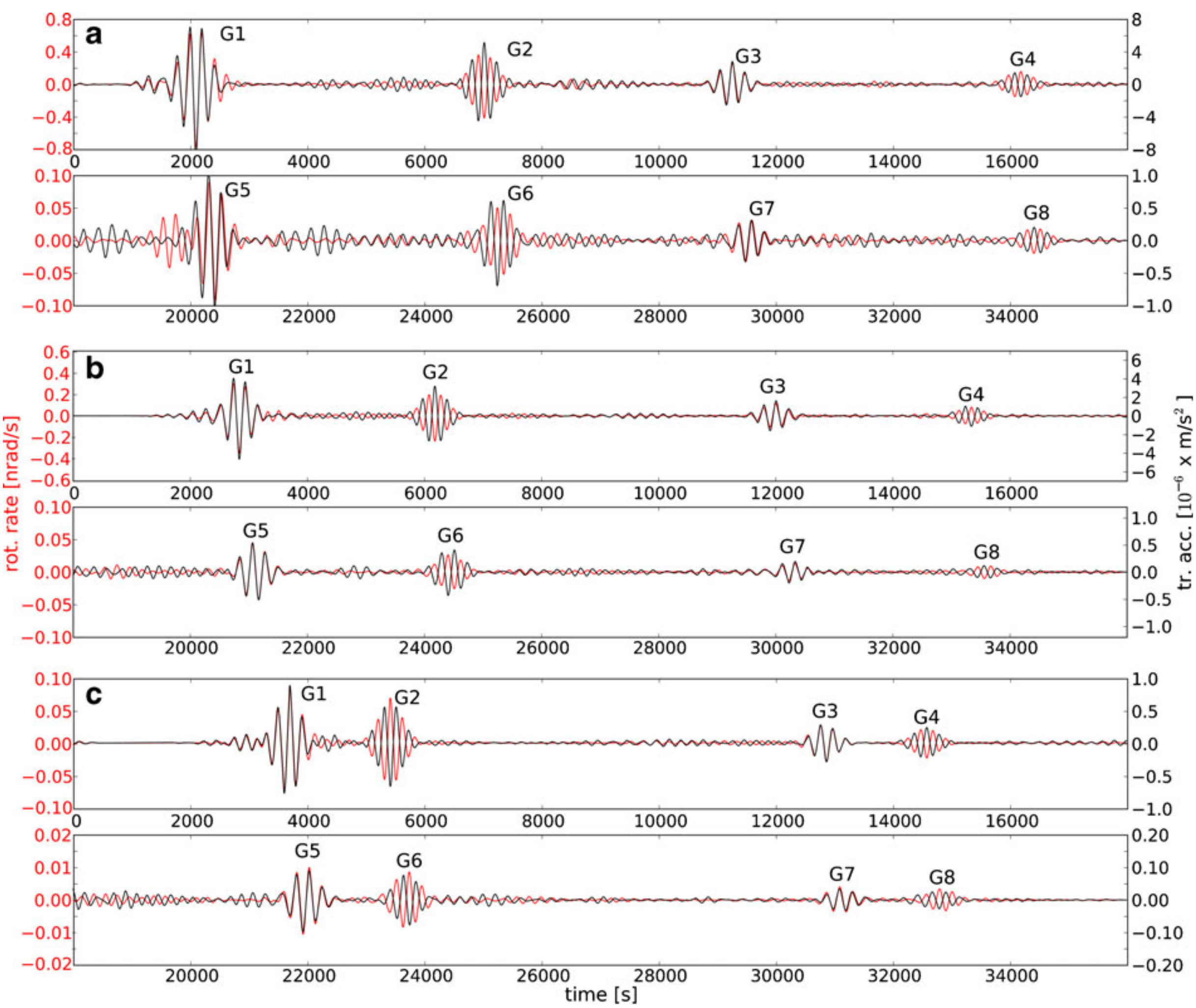

Fig. 3 Same as Fig. 2 but for synthetic seismograms calculated using mode summation with the PREM Earth model and Global CMT source parameters

Table 2 Phase velocities of Love waves for data and synthetics generated by the Tohoku (2011), Chile (2010) and Samoa (2009) earthquakes, calculated as one half of the ratio between horizontal–transverse acceleration and the rotational rate

Event	Phase velocity Data [km/s]	Phase velocity Synthetics [km/s]	Difference %
Tohoku	5.2	4.7	−9.6
Chile	4.6	4.9	+6.5
Samoa	5.1	4.7	−7.8

2010), transverse accelerations and rotation rate around a vertical axis are expected to be in phase for SH waves (that is, to have identical waveforms) and the ratio of their amplitudes scales with phase velocity for plane wave propagation.

The seismograms were band-pass filtered with a "zero-phase Butterworth" filter (between 180 and 280 s). The polarity of the superimposed ground motion components shown in Fig. 2 is adjusted so that G1 (the Love wave propagating through the minor arc) correlates positively. Since the rotational wave field is proportional to the wave number vector (*k*) (Ferreira and Igel 2009), it depends on the propagation direction. Therefore, the polarity is reversed for all the major-arc waves (G_{2n}) because they travel on the opposite direction from the first arrival.

Synthetic seismograms for rotation rate and transverse acceleration were calculated by normal mode summation (Fig. 3). Synthetic computations were done with the Mineos code (Masters et al. 2007) for a spherically symmetric PREM model (Dziewonski and Anderson 1981) and earthquake source parameters from the Global Centroid moment tensor catalogue (Dziewonski et al. 1981). The reverse polarity for the G_{2n} waves is also observed in synthetic seismograms, as expected, and the amplitudes are in a good agreement with the data. We calculated phase velocities of the Love waves for both synthetics

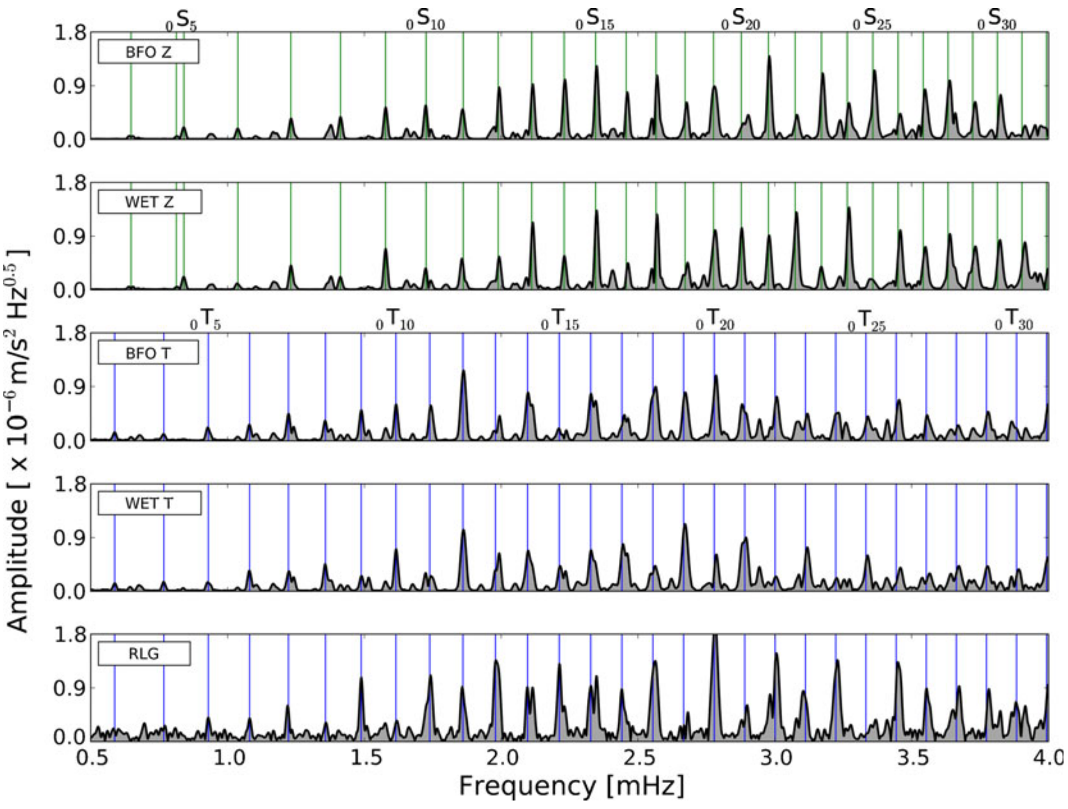

Fig. 4 Observed power spectral density (PSD) for a 36-h time window following the Tohoku earthquake on February 2011. From the *top* to the *bottom*, vertical component spectra recorded at BFO and WET, transverse component spectra for BFO and WET and the G-ring laser RLAS (multiplied by a factor of 10,000). *Vertical lines* indicate frequencies computed for the PREM model of the fundamental spheroidal modes (vertical component translations; *green*) and toroidal modes (transverse component and rotations; *blue*)

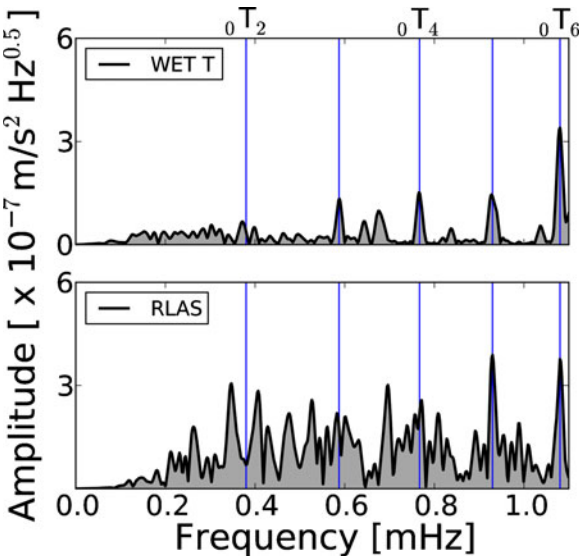

Fig. 5 Spectral noise level comparison between horizontal transverse acceleration by station WET (*top*) and rotational rate by the G-ring RLG (*bottom*)—multiplied by a factor of 10,000—for a 36-h time window following the Tohoku earthquake. *Vertical lines* indicate frequencies of fundamental toroidal modes for the PREM model

and data and represented them as one half of the ratio between the peak amplitudes of each G_n wave for translations and rotations.

The average over the phase velocities from each Love wave arrival is calculated for each event in a frequency range between 3.6 and 5.6 mHz (280 to 180 s). Noting the influence of the path and the local structure beneath the receiver (Ferreira and Igel 2009), the results are in the range of the expected values, with a differential percentage between 6.5 and 9.6 % for phase velocities between data and synthetics as is shown in Table 2.

As expected, the amplitude of the waves for all the events decreases as they orbit the Earth (at the same rate for rotation and translation), and the waveforms remain similar even for high-orbit Love waves. However, for the event in Chile, Love waves G2 and G6 show slightly smaller amplitude than G3 and G7, respectively. This is probably due to focusing and defocusing by lateral heterogeneity along those particular paths. Rotational and translational motions show similar sensitivities to such heterogeneities.

Moreover, the amplitude of rotations for Love wave G6 is smaller than the transverse acceleration

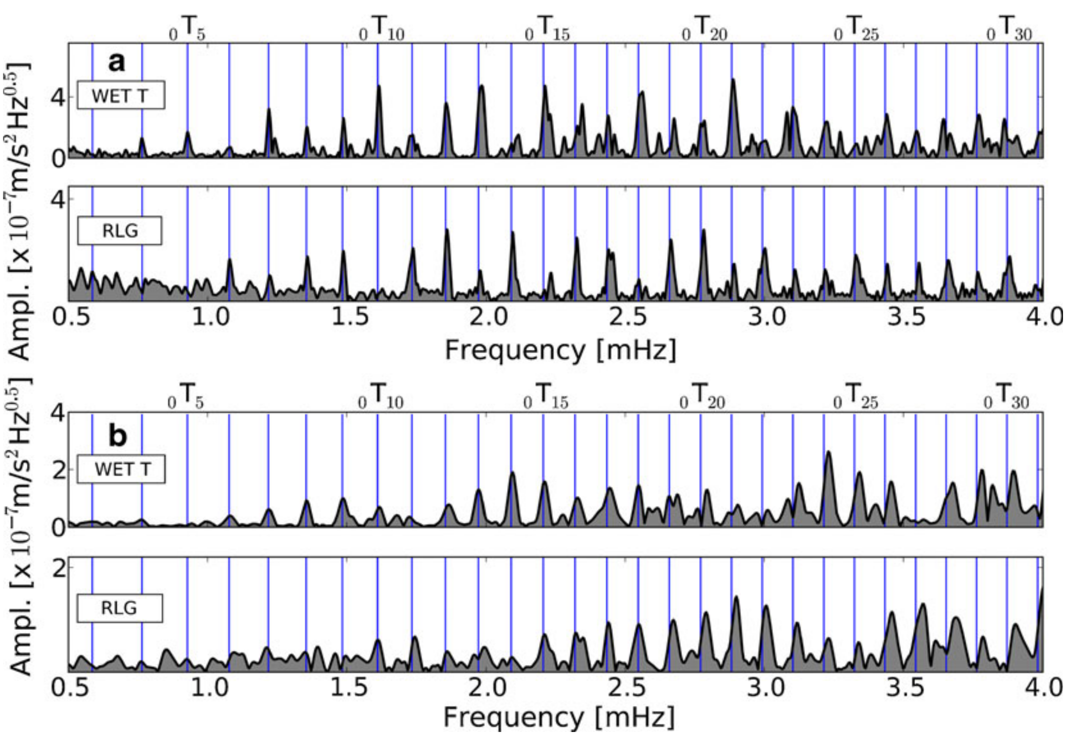

Fig. 6 Observed PSD of the **a** Chile event for time series of 36 h and **b** Samoa event for a time series of 16 h recorded for horizontal transverse acceleration by station WET (*top*) and rotational rate by the G-ring RLG (*bottom*) multiplied by a factor of 10,000. *Vertical lines* indicate frequencies of fundamental toroidal modes for the PREM model

compared to other Love waves. This difference suggests that rotational motions are more sensitive to focusing and defocusing in this case. Since lateral heterogeneity is not taken into account in the synthetics shown in Fig. 3, focusing and defocusing effects do not appear in the synthetics.

3.2 Frequency-domain observations and modelling

We computed power spectral densities (PSDs) for the toroidal free oscillations excited by the three events. Once again, we compared records of transverse acceleration at WET to rotations of the G-ring RLG.

Ideally, for normal mode observations, the longer the time window used, the better the peak resolution is. However, the noise level increases with time as well, and we found that a time series of 36 h from onset provided the best available trade-off for the Tohoku and Chile earthquakes. For the Samoa earthquake, we reduced that window to 16 h to exclude seismic waves from another strong event (M_W 7.5, near the coast of Sumatra). In spite of the shorter time window, the normal mode peaks can be identified.

Data processing included (1) correction for the instrument response; (2) application of a Hanning (von Hann) taper; (3) a high-pass filter with corner frequency

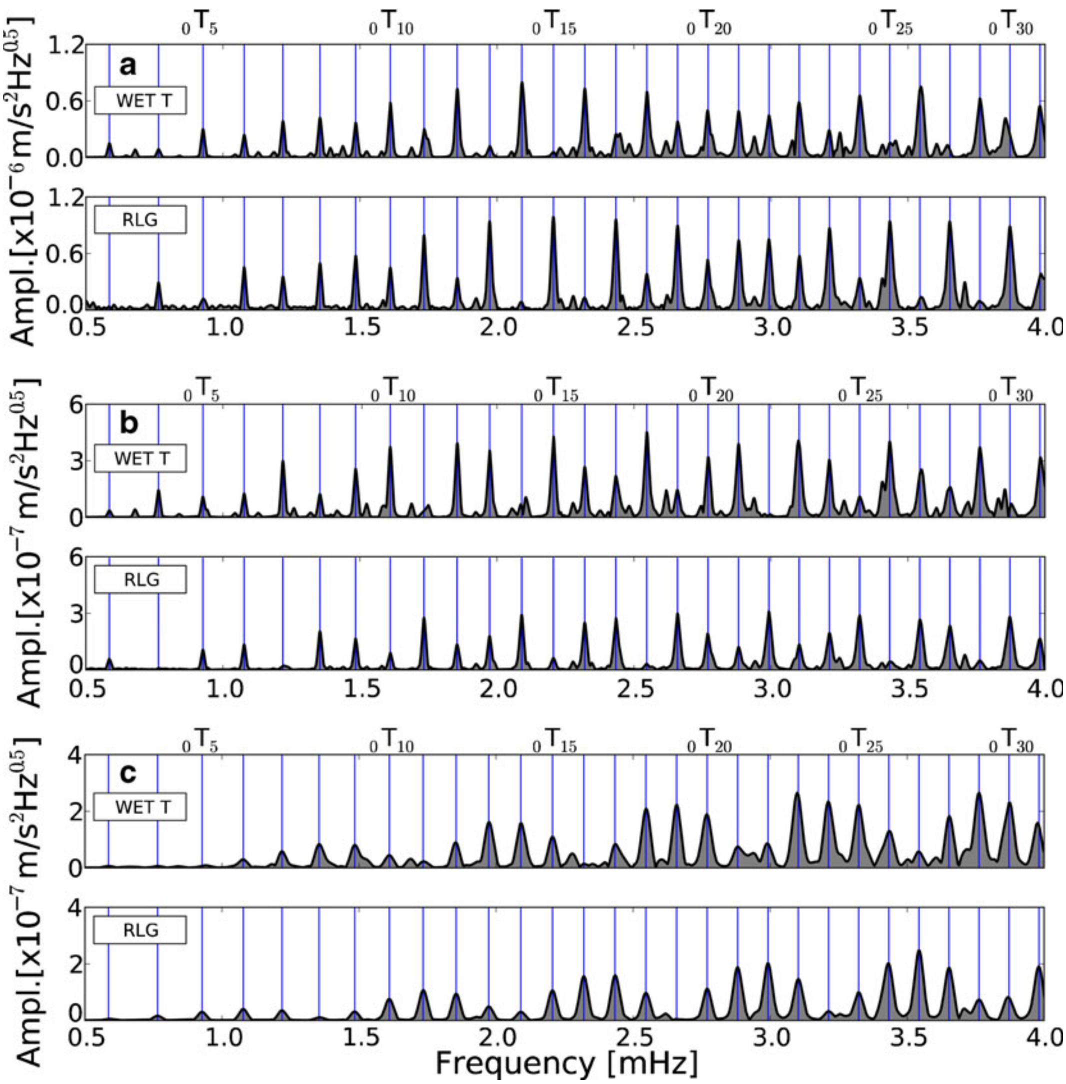

Fig. 7 Same as Fig. 5 but for synthetics seismograms of a 36-h record of the **a** Tohoku and **b** Chile events and **c** a 16-h record of the Samoa event

of 0.3 mHz and (4) computing the spectra via Fourier transform. For comparison, we also analysed data recorded with a set of STS-1 seismometers at the Black Forest Observatory (BFO) for the Tohoku event. BFO is about 350 km west of Wettzell (Fig. 4) and is known to be one of the world's quietest observatories for the long-period seismic signals (Richter et al. 1995).

Spheroidal modes detected in the vertical translational components at BFO and WET display comparable PSDs up to a frequency of 2 mHz (500 s), where the corresponding wavelength is much larger than the distance between the stations. For toroidal modes, a comparison between WET and BFO leads to the same conclusions as those for the vertical component. Nevertheless, when comparing WET translational and RLG spectra, substantial differences are seen for the Tohoku event, despite the fact that the instruments are collocated (Igel et al. 2011).

Figure 5 shows in detail the behaviour of the G-ring RLG spectra from 0 to 1.1 mHz in order to evaluate the background noise level of the instrument in comparison with the WET broadband station. From the figure, one can see that the performance of the G-ring RLG in this frequency band is still not as good as the STS-2 stations. Therefore we focus on frequencies higher than 1 mHz.

The observed transverse acceleration and rotational rate spectra for the Chile and the Samoa earthquakes are shown in the Fig. 6. In common between the events, one can identify contrasting amplitudes between rotations and translations—large spectral amplitudes in translation correspond to small amplitudes in rotations and vice versa.

This contrasting pattern is uneven, meaning that it was not observed for every mode. For the Tohoku event spectra, this behaviour is clear, for example, for the mode ${}_0T_{10}$ (a comparatively large amplitude in rotation and small amplitude in the transverse component) and vice versa for the mode ${}_0T_{19}$. Since the wave trains G_{2n} are anti-correlated for the two observables, it is natural that as a result the corresponding rotation and acceleration spectra will be different (as normal modes can be seen as resulting from the interference of multiple-orbit surface waves).

A slight difference from the eigenfrequencies predicted by PREM was observed in the spectra of all three events. This deviation increases with the frequency and may be due to the effect of the Earth's rotation, the ellipticity of the figure and lateral variations in density and elastic parameters. For a better understanding of these observed differences between the translational and rotational PSD amplitudes, we computed synthetic spectra for the events (Fig. 7).

These synthetic amplitudes are in reasonably good agreement with the observations, given the simplicity of the model we used; the synthetic seismograms have the same relative-amplitude behaviour between rotations and translation for some modes. Rotation rates in the surface of the Earth are defined in the frequency

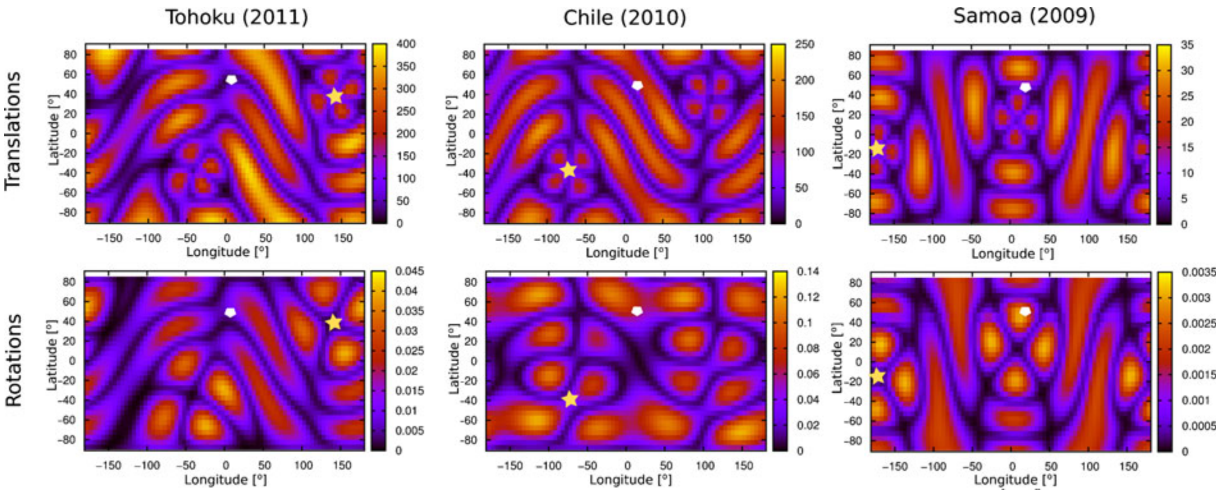

Fig. 8 Synthetic translational and rotational motions for toroidal free oscillations for the Tohoku (2011), Chile (2010) and Samoa (2009) events (*stars*) and Wettzell station (*white dots*). Displacement (*top*) and rotation fields (*bottom*) for toroidal mode ${}_0T_5$ as a function of latitude and longitude

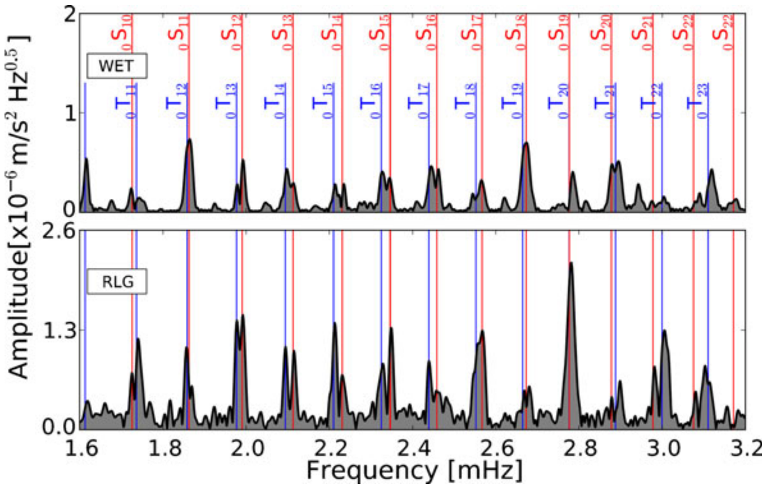

Fig. 9 Spectra for 48 h of data following the Tohoku event. Comparison of observed coupled modes between transverse acceleration records at WET (*top*) and rotations around the vertical from the G-ring RLG (*bottom*) (multiplied by a factor of 10,000). *Vertical lines* indicate frequencies of fundamental spheroidal (*red*) and toroidal (*blue*) modes for the PREM model

domain as the curl of the translational velocity spectrum for a given mode of vibration ω_m^{ℓ}. Therefore, one expects that the superposition of the standing waves leads to different nodal lines along the Earth for each type of motion.

To understand the characteristics of toroidal mode spectra for horizontal displacement and rotation rate, we carried out a synthetic calculation of the complete oscillation field of rotations and translations over the globe. We computed the frequency-domain amplitude of a single toroidal mode, ${}_0T_5$, for rotation and displacement in each station located at 5 ° distance (Fig. 8). A double-couple source radiation pattern is seen in both observables. Since the focal mechanisms of the earthquakes differ, they have different energy distributions.

For all three events, one can see spatial differences between the rotational and transverse fields. Upon the location of the station, these differences range from considerable to imperceptible. Focusing on the receiver location in Germany (white dot in Fig. 8), contrasting motions of ${}_0T_5$ for rotation and translation are observed for the Tohoku and Samoa events. On the other hand, this feature is not perceptible for the event in Chile. This variation can also be seen in Fig. 7, confirming that it is a geometric effect depending on the number of nodal lines generated by the mode, the source–receiver distance and the source radiation pattern.

3.3 Coupled modes

In the real Earth, normal mode spectra become more complex due to the Earth's daily rotation, its hydrostatic ellipticity and structural heterogeneity. As a consequence of deviations from a spherically symmetric,

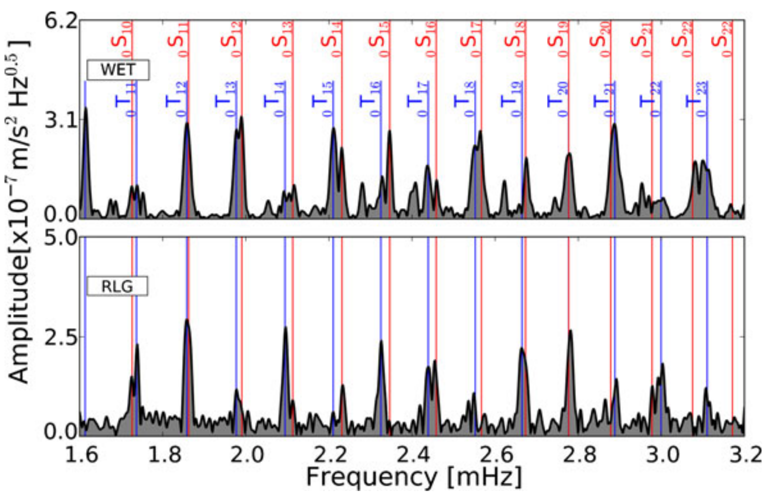

Fig. 10 Same as Fig. 8 but for the 2010 Chile earthquake

non-rotating, perfectly elastic, isotropic Earth model, one observes splitting of the eigenfrequencies in their azimuthal order as well as coupling between modes. In the range of our mode observations, coupling between modes due to Coriolis forces is the dominant effect (Masters et al. 1983).

In Figs. 9 and 10, PSDs for 48 h of data following the Tohoku and the Chile events are shown; the processing is the same as described above. Spheroidal eigenfrequencies are present in the rotational and in the acceleration spectra, and these may be due to Coriolis coupling between fundamental spheroidal and toroidal modes, ${}_nS_\ell$ and ${}_nT_{\ell+1}$.

Once again, the comparison with the transverse acceleration spectra shows substantial variation between events. For some modes, it seems that one mode type (${}_nS_\ell$ or ${}_nT_\ell$) dominates in amplitude, but in some cases that dominant mode, in coupled modes, differs between acceleration and rotation spectra. For example, in Fig. 9 the coupled mode ${}_0S_{14}$–${}_0T_{15}$ has a stronger toroidal contribution in the G-ring RLG observation, while in the translational spectra spheroidal and toroidal eigenfrequencies have similar amplitudes.

On the other hand, the coupled mode ${}_0S_{12}$–${}_0T_{13}$ has dominant spheroidal energy in the acceleration spectra rather than in rotational spectra, indicating that mode coupling may be asymmetric between rotations and translations. This issue deserves further investigation. We are currently carrying out work towards the calculation of more sophisticated rotational spectra simulations.

4 Conclusions

We show that the systematic observation with the G-ring RLG of torsional normal modes is possible for earthquakes of moment magnitude $M_W \geq 8.0$. Our observations are in good agreement with synthetic calculations for the PREM model.

The high sensitivity of this instrument allows us to observe possible coupling between modes in the frequency band between 1.6 and 3.2 mHz (625 to 313 s). Nevertheless, the effects generating such coupling need to be investigated further. Our observations demonstrate that rotational-motion measurements are complementary to standard translational measurements in long-period seismology studies.

Acknowledgments A special thank-you goes to those who contributed to this paper: Kostas Lentas for his help in benchmarking the synthetic study on the High Performance Computing Cluster supported by the Research Computing Service at the University of East Anglia. Walter Zürn and an anonymous reviewer for their constructive comments and helpful suggestions. Also we extend our heartfelt gratitude to Dr. John R. Evans for his great support editing the paper. We acknowledge support from the European Commission (Marie Curie Actions, ITN QUEST, www.quest-itn.org) and the German Research Foundation (Project Ig16/8).

References

Beghein C, Trampert J (2003) Robust normal mode constraints on inner core anisotropy from model space search. Science 299:552–555

Deuss A, Irving JCE, Woodhouse JH (2010) Regional variation of inner core anisotropy from seismic normal mode observations. Science 328:1018–1020

Dziewonski AM, Anderson D (1981) Preliminary reference Earth model. Phys Earth Planet Inter 25:297–356

Dziewonski AM, Chou TA, Woodhouse JH (1981) Determination of earthquake source parameters from waveform data for studies of global and regional seismicity. J Geophys Res 86:2825–2852

Ferreira AMG, Igel H (2009) Rotational motions of seismic surface waves in a laterally heterogeneous earth. Bull Seismol Soc Am 99:1429–1436

Giardini D, Li EX, Woodhouse JH (1987) Three dimensional structure of the earth from splitting in free oscillation spectra. Nature 325:405–411

Gilbert F, Dziewonski AM (1975) An application of normal mode theory to the retrieval of structural parameters and source mechanisms from seismic spectra. Phil Trans R Soc Lond 278:187–269

Igel H, Cochard A, Wassermann J, Flaws A, Schreiber U, Velikoseltsev A, Pham DN (2007) Broad-band observations of earthquake-induced rotational ground motions. Geophys J Int 168(1):182–196

Igel H, Nader MF, Kurrle D, Ferreira AM, Wassermann J, Schreiber KU (2011) Observations of Earth's toroidal free oscillations with a rotation sensor: the 2011 magnitude 9.0 Tohoku-Oki earthquake. Geophys Res Lett. doi:10.1029/2011GL049045

Ishii M, Tromp J (1999) Normal-mode and free-air gravity constraints on lateral variations in velocity, and density of the Earth's mantle. Science 285:1231–1236

Kurrle D, Igel H, Ferreira AMG, Wassermann J, Schreiber U (2010) Can we estimate local Love wave dispersion properties from collocated amplitude measurements of translations and rotations? Geophys Res Lett 37 (L04):307

Laske G, Masters G (1999) Limits on differential rotation of the inner core from analysis of earths free oscillations. Nature 402:66–69

Masters, G., Park, J., and Gilbert, F. (1983) Observations of coupled spheroidal and toroidal modes, J. Geophys. Res. 88(B12), 10,285–10,298

Masters G, Barmine M, Kientz S (2007) Mineos: user manual. Calif. Inst. Technol, Pasadena

Pancha A, Webb TH, Stedman GE, McLeod DP, Schreiber U (2000) Ring laser detection of rotations from teleseismic waves. Geophys Res Lett 27:3553–3556

Pham ND, Igel H, Wassermann J, Cochard A, Schreiber U (2009) The effects of tilt on interferometric rotation sensors. Bull Seismol Soc Am 99(2B):1352–1365

Richter B, Wenzel HG, Zürn W, Klopping F (1995) From Chandler wobble to free oscillations: comparison of cryogenic gravimeters and other instruments in a wide period range. Phys Earth Planet Inter 91:131–148

Schreiber U, Stedman G, Igel H, Flaws A (2006) Ring laser gyroscopes as rotation sensors for seismic wave studies. In: Teisseyre R, Takeo M, Majewski E (eds) Earthquake source asymmetry, structural media and rotation effects. Springer, Berlin, pp 391–402

Schreiber U, Hautmann JN, Velikoseltsev A, Wassermann J, Igel H, Otero J, Vernon F, Wells JPR (2009) Ring laser measurements of ground rotations for seismology. Bull Seismol Soc Am 99(2B):1190–1198

Widmer-Schnidrig R, Zürn W (2009) Perspectives for ring laser gyroscopes in low-frequency seismology. Bull Seismol Soc Am 99(2B):1199–1206